Journal of Power Sources 196 (2011) 5095–5101

Contents lists available at ScienceDirect

Journal of Power Sources

journal homepage: www.elsevier.com/locate/jpowsour

Enhanced hydrogen generation by hydrolysis of $LiBH_4$ doped with multiwalled carbon nanotubes for micro proton exchange membrane fuel cell application

Baicheng Weng*, Zhu Wu, Zhilin Li, Hui Yang, Haiyan Leng

Shanghai Institute of Microsystem and Information Technology, Chinese Academy of Sciences, PR China

ARTICLE INFO

Article history:
Received 25 December 2010
Received in revised form 26 January 2011
Accepted 27 January 2011
Available online 2 February 2011

Keywords:
Lithium borohydride
Hydrolysis
Proton exchange membrane fuel cell
Hydrogen generation
Carbon nanotubes

ABSTRACT

$LiBH_4$ has a high hydrogen storage capacity and could potentially serve as a superior hydrogen storage material. However, during the hydrolysis process for hydrogen generation, the agglomeration of the hydrolysis product of $LiBH_4$ limits its full utilization. In order to completely release the stoichiometric amount of H_2 from $LiBH_4$ hydrolysis, multiwalled carbon nanotubes (MWCNTs) were doped with $LiBH_4$ by mechanical milling. The results show that MWCNT carried $LiBH_4$ can slowly react with water vapor at room temperature which is 25 °C lower than the reaction temperature of neat $LiBH_4$. Agglomeration can be avoided when the addition of MWCNTs exceeds 7 wt.%, which results in a complete hydrolysis process. The total hydrogen capacity is 7.5 wt.%. The enhanced hydrolysis of $LiBH_4$ can be attributed to the MWCNTs which increased the contact areas between $LiBH_4$ and water and created gas channels for hydrogen diffusion. The performance of a micro proton exchange membrane fuel cell connected to MWCNT-doped $LiBH_4$ powder packed-bed reactor was examined. The result demonstrates that doping with MWCNTs enhanced the hydrogen generation of $LiBH_4$ hydrolysis. MWCNT-doped $LiBH_4$ can be applied as hydrogen source of fuel cells.

1. Introduction

Proton exchange membrane fuel cells (PEMFCs) are finding extensive use in applications ranging from small electronic devices to medium-sized stationary power generators [1–4]. In order to fuel the PEMFCs, a source of hydrogen is required. Taking into account both hydrogen related components and safety requirements, it is necessary to have a hydrolysable hydride with at least 10 wt.% hydrogen capacity [5].

Lithium borohydride ($LiBH_4$) has high gravimetric (18.5 wt.%) and volumetric (121 kg m^{-3}) capacities of hydrogen and can potentially serve as a good hydrogen storage material [6–13]. However, thermodynamic and kinetic limitations caused by strong covalent and ionic bonds greatly restrained the practical application of $LiBH_4$ as a reversible hydrogen storage material. In contrast, the hydrolysis of $LiBH_4$ is of interest for the generation of H_2 [14]. Kojima et al. [14] found that the gravimetric and volumetric hydrogen densities increased with increasing $H_2O/LiBH_4$ ratio, and reached the maximum values of 7.4 wt.% and 60 kg m^{-3} at $H_2O/LiBH_4$ ratio of 3:1 (mol/mol), respectively. However, Laversenne et al. [15] compared hydrolysis conditions of $LiBH_4$, $NaBH_4$ and KBH_4, and found that the hydrolysis product of $LiBH_4$ was different at different temperatures. $LiBO_2{\cdot}2H_2O$ is generated at temperatures below 120 °C while $LiBO_2{\cdot}(1/3)H_2O$ is generated at temperatures above 255 °C, which indicates that the hydrogen yield will vary at different temperatures. Therefore, the hydrolysis process of $LiBH_4$ still needs further investigation. Kong et al. [16] indicated that $LiBH_4$ did not react with water vapor at room temperature. Zhu et al. [17] found that the hydrolysis reaction of $LiBH_4$ was fast, but never produced more than 50% of its theoretical yield because the products form a solid and impermeable mass clogging the reaction vessel, thus limiting the full utilization of the hydride. In this regard, the complete hydrolysis of $LiBH_4$ is desirable.

In this paper, we first investigated the hydrolysis of $LiBH_4$ and then presented a novel strategy for completely hydrolyzing $LiBH_4$ to provide hydrogen for PEMFCs by the addition of MWCNTs. Choosing MWCNTs as an additive is motivated by the recent findings that MWCNTs are highly effective for improving the power outputs of borohydride fuel cell and the dehydrogenation performance of $LiBH_4$ due to the high effective surface area and catalytic activity [18,19]. Furthermore, MWCNTs are porous materials which can disperse $LiBH_4$ to avoid the agglomeration effect. Finally, a $LiBH_4$/MWCNT powder packed-bed reactor was connected to a silicon-based micro electromechanical system (MEMS) PEMFC, and the performance of the system, such as polarization curve and power density plot was presented.

* Corresponding author. Tel.: +86 21 62511070; fax: +86 21 32200534.
E-mail address: bcweng@mail.sim.ac.cn (B. Weng).

0378-7753/$ – see front matter © 2011 Elsevier B.V. All rights reserved.
doi:10.1016/j.jpowsour.2011.01.080

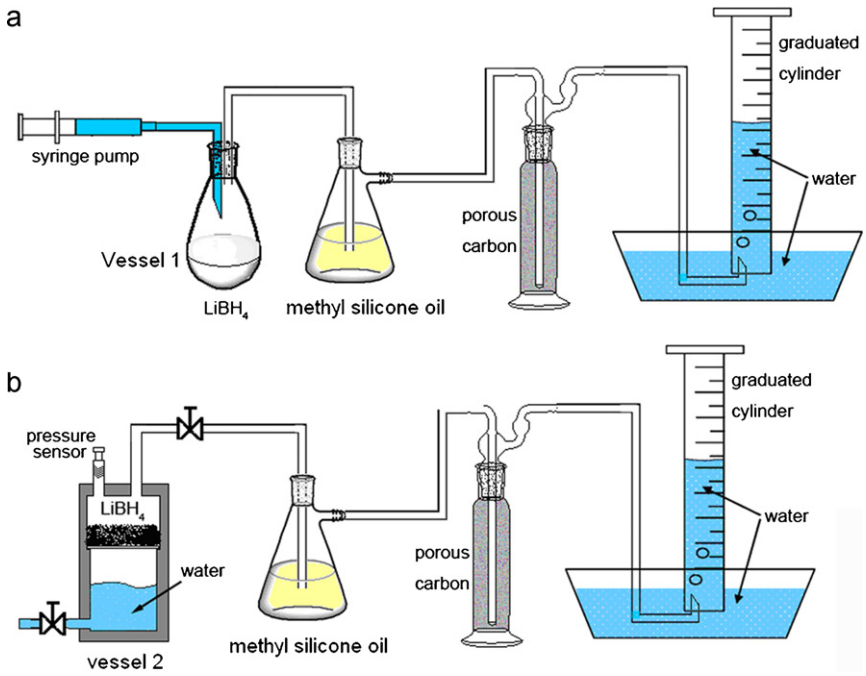

Fig. 1. Schematic diagram of the experimental apparatus used to measure the hydrogen generation from hydrolysis of $LiBH_4$ with liquid water (a) and water vapor (b).

2. Experimental

2.1. Materials and characterization

Lithium borohydride ($LiBH_4$, 95% purity) was purchased from Sigma–Aldrich Chemical Company. MWCNTs were purchased from Shenzhen Nanotech Port Co. Ltd. The diameters of the MWCNTs are 10–20 nm with the length ranging from 10 to 15 μm. All sample handling was performed in MBraun Labmaster 130 glove box maintained under argon atmosphere with <1 ppm O_2 and H_2O vapor.

The samples of $LiBH_4$ doped with different amounts of MWCNTs (0 wt.%, 3 wt.%, 5 wt.%, and 7 wt.%) were prepared by mechanical milling using a Fritsch Pulverisette 6 planetary ball mill (PBM) at 150 rpm for 30 min under Ar atmosphere. The milling pot is made of hardened steel with 50 mL in volume and the ball-to-powder weight ratio is 30:1.

X-ray diffraction measurements were carried out by a Rigaku D/max 2400 using Cu/Kα radiation. Samples were mounted onto a 1 mm depth glass board and sealed with a polyvinylchloride membrane to avoid oxidation during the XRD measurements. ^{11}B magic-angle-spinning nuclear magnetic resonance (MAS-NMR) experiments were carried out at room temperature on a Bruker Advance 300 NMR spectrometer (Bruker, German) operating at 9.7 T on 128.3 MHz. Spectra were obtained using a two-channel custom-built probe with a 3 mm ZrO_2 rotor, and the magic-angle-spinning rate was set to 5 kHz to avoid the overlapping of spinning sidebands on other resonance lines. 300 scans were taken for the samples. The chemical shift was referred to $NaBH_4$ (−41 ppm). The electrochemical characterization was tested using a Solartron SI 1287 potentiostat (Solartron Analytical, Hampshire, UK). All the tests were performed at room temperature. Morphology of the hydrolysis products was characterized by a field emission scanning electron microscopy (FESEM, HITACHI S4700, Japan) using an acceleration voltage of 100 kV.

2.2. Apparatus and procedures

A schematic diagram of the experimental setup used to measure the hydrogen generation is shown in Fig. 1. The apparatus consisted

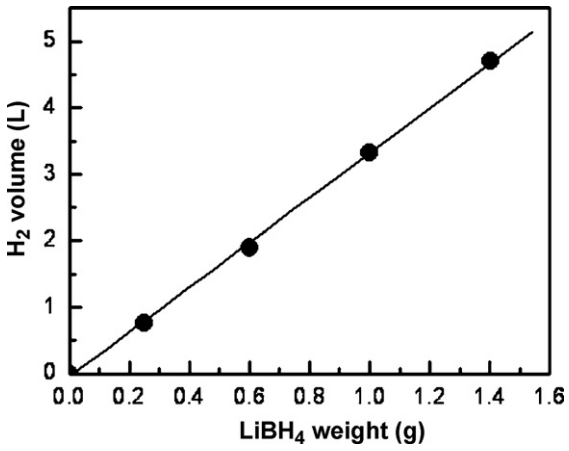

Fig. 2. Hydrogen generation profile of $LiBH_4$ hydrolysis.

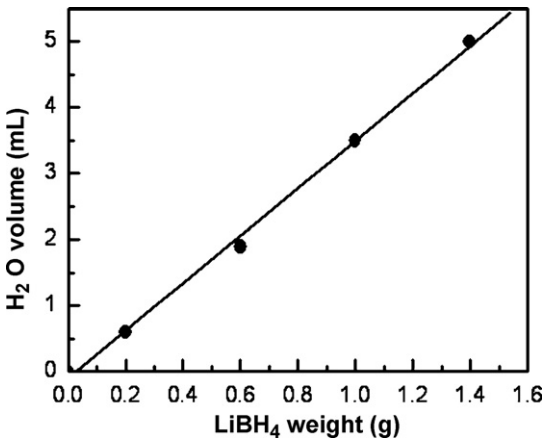

Fig. 3. The dependence of water consumed on the weight of $LiBH_4$.

of a small reaction vessel, a syringe pump, and a water trap. Two types of reactors were designed. Reaction vessel 1 is made of glass. It was designed for the reaction of $LiBH_4$ with liquid water, which was sealed by two plugs: a water inlet plug and a hydrogen outlet plug with a central hole covered with a porous carbon filter. The volume of the reaction vessel is 100 mL. Reaction vessel 2 is made of stainless steel. It was sealed by two valves. As shown in Fig. 1b, the first valve was set on the vessel bottom for water inlet which was closed after water injection. The second valve was for hydrogen outlet. The syringe pump was used to deliver water into the vessel to react with the hydrides. The generated hydrogen gas was collected and its volume was measured in the water trap, which consists of an inverted water-filled 500 mL graduated cylinder immersed in a water tray, and interconnected with the reactor by PVC tubing.

In order to characterize the reaction between $LiBH_4$ and water at room temperature, we measured the amount of hydrogen generated and the amount of water consumed. Water was pumped directly into the vessel, and the generated hydrogen was measured by a graduated cylinder and calculated according to the ideal gas equation by referring the molar value of $LiBH_4$ as 1 equivalent (abbr. as equiv.). The consumed water was regarded as the amount of water for hydrolyzing $LiBH_4$. To obtain accurate results, a series of H_2 and water amounts were measured by hydrolyzing various amounts of $LiBH_4$ powders, and the equivalent values of generated H_2 and consumed water were determined by fitting the experimental data into a linear equation. The kinetics of the hydrolysis of $LiBH_4$ was also measured at different flow rates of water injected by a micro syringe pump.

The temperature changes during the hydrolysis of $LiBH_4$ were measured by infrared temperature measurement device.

3. Results and discussion

3.1. Hydrolysis process of $LiBH_4$

In order to characterize the hydrolysis process of $LiBH_4$, deionized water was directly pumped into the reactor using a micro pump at a flow rate of 10 μL h^{-1} until no hydrogen was generated. To reduce the effect of clogging by solid mass which would prevent the continuous reaction of $LiBH_4$ with water, the suspension was dispersed by ultrasonic vibration during the hydrolysis process. The hydrogen yield in molar calculated by the state equation of ideal gas from $LiBH_4$ hydrolysis volumetric amount (Fig. 2) is 3.6 equiv., which is close to the theoretical value (3.8 equiv. for 95% $LiBH_4$, hydrogen yield decrease is attributed to oxidation and impurity of $LiBH_4$) according to the following reaction which is postulated by Schlesinger et al. [20] as real reaction process of $LiBH_4$ hydrolysis:

$$LiBH_4 + 2H_2O \rightarrow LiBO_2 + 4H_2 \quad (1)$$

Fig. 3 shows the amount of water required to fully hydrolyze $LiBH_4$. As shown in Fig. 3, 4.3 equiv. of water is required for the hydrolysis reaction. The XRD result of hydrolysis product is shown in Fig. 4, and all diffraction peak positions are listed in Table 1. The result clearly shows the hydrolysis product of $LiBH_4$ comprises only one compound $LiBO_2{\cdot}2H_2O$. Therefore, the reaction process can be described as follows:

$$LiBH_4 + 4.3H_2O \rightarrow LiBO_2{\cdot}2H_2O + 4H_2 + 0.3H_2O \quad (2)$$

The above results demonstrate that under the effect of ultrasonic dispersion, 1 equiv. $LiBH_4$ reacting with 4.3 equiv. water leads to 4 equiv. hydrogen release. The total hydrogen yield (taking hydrate into account) is 8.0–8.1 wt.%, which is higher than 5.8 wt.% for NH_3BH_3 [21] and 7.2 wt.% for $NaBH_4$ [22].

It can be seen from the reaction (2) that water consumption in our experiment is higher than the theoretical value. To further understand the phenomena, the maximum temperature during hydrolysis process with different $LiBH_4$ bulk densities and stoichiometric amounts of water was measured. As shown in Fig. 5, the result suggests that the maximum temperature increased from room temperature to 84 °C during the hydrolysis. With the bulk density of $LiBH_4$ increasing to 0.33 g cm^{-3}, the maximum temperature also rises slowly to 97 °C, and then with the bulk density increasing further, the maximum temperature rises rapidly and reaches 184 °C at the bulk density of 0.54 g cm^{-3} which is near the real density of $LiBH_4$. These results indicate that water tends

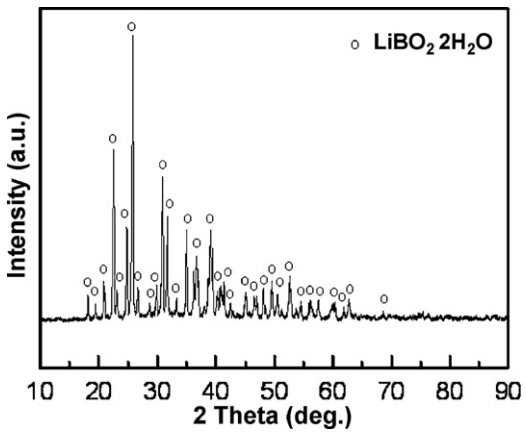

Fig. 4. XRD pattern of solid product of $LiBH_4$ hydrolysis.

Table 1
Peak positions for phases observed in Fig. 4.

Phase	Peak position	Reference
$LiBO_2{\cdot}2H_2O$	18.103, 19.456, 20.895, 22.523, 24.721, 25.642, 26.695, 29.780, 30.897, 31.609, 33.127, 34.931, 36.201, 36.693, 36.801, 38.683, 39.069, 39.207, 40.217, 40.830, 41.309, 42.464, 45.063, 45.516, 46.929, 48.074, 48.406, 49.455, 50.069, 50.350, 51.115, 52.510, 53.740, 54.530, 56.010, 57.397, 59.759, 60.249, 61.801, 62.707	This work
$LiBO_2{\cdot}2H_2O$	18.033, 19.303, 20.787, 22.353, 24.679, 25.541, 26.528, 29.689, 30.718, 31.518, 33.06 34.857, 36.109,36.532, 36.765, 38.567, 38.878, 39.183, 40.144, 40.913, 41.214, 42.314, 44.942, 45.517, 46.824, 47.929, 48.386, 49.423, 49.9, 50.255, 51.118, 52.477, 53.592, 54.39, 55.954, 57.271, 59.742, 60.164, 61.74, 62.667	PDF#44-0419

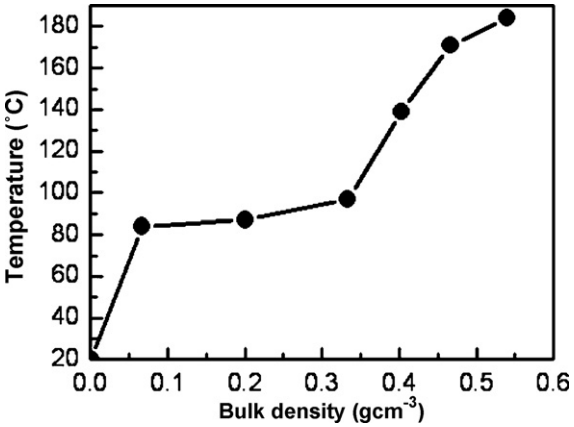

Fig. 5. Relationship between the maximum temperature in the reactor during $LiBH_4$ hydrolysis with different $LiBH_4$ bulk densities and stoichiometric amounts of water.

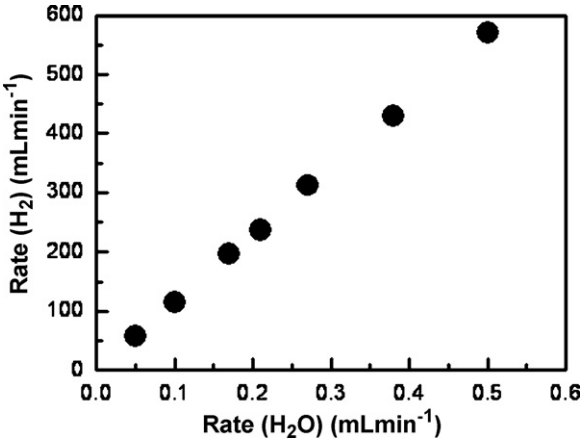

Fig. 6. The dependence of hydrogen generation rate on water injection velocity.

to be vaporized during the hydrolysis, and water vapor can be partially carried away from the vessel with hydrogen, which can explain the result that an extra 0.3 equiv. water is required to completely hydrolyze $LiBH_4$. Kojima et al. [14] has demonstrated that in the case of using a stoichiometric amount of water, the temperature of the hydrolysis system shows the maximum value of 120 °C at 10 s after water injection, and decreases rapidly with time. In our experiments, the temperature of the reaction vessel is depended not only on the chemical properties of $LiBH_4$, but also on the heat diffusion. Because higher bulk density means less space for heat diffusion, with the increase of the bulk density of $LiBH_4$, the temperature of the vessel rises as shown in Fig. 5, which affected the water consumption and hydrolysis product.

Fig. 6 shows the dependence of hydrogen generation rate on water injection velocity. The result shows that hydrogen release rate rises with the increase of water injection velocity. With water injection velocity ranging from 0.05 to 0.5 mL min^{-1}, hydrogen generation rate ranges from 50 to 600 mL min^{-1}, which indicates that hydrogen is generated from $LiBH_4$ hydrolysis at fast rate. According to these results, $LiBH_4$ can quickly and fully hydrolyze if the side effect of clogging by solid mass can be avoided. $LiBH_4$ represents a promising hydrogen production medium with the highest H_2 yield for fuel cell applications.

3.2. *Effect of MWCNTs on the kinetic performance of $LiBH_4$ hydrolysis*

To study the clogging effect of $LiBH_4$ hydrolysis, the reaction of $LiBH_4$ doped with different amounts of MWCNTs with water vapor was investigated by the following experiment. A home-made cylinder vessel with a stainless steel sieve (1000 openings/in., surface area 5 cm^2) to isolate reactant powder from water was used in the experiments as shown in Fig. 1b. Plain $LiBH_4$ or $LiBH_4$/MWCNT mixture as reactant was put in the stainless steel sieve, and then the cylinder vessel was tightly sealed. All operations were conducted in a glove box. Excess liquid water was injected into the vessel, and enough space was left between water and the sieve, so liquid water was not in direct contact with the hydride. Then the vessel was heated up to 80 °C at a heating rate of 0.5 °C min^{-1}. The reaction between water vapor and $LiBH_4$ was first initiated at the bottom of the hydride powder. Clogging by the hydrolysis product prevented $LiBH_4$ on the top of the product from reacting with water vapor. Fig. 7a shows the hydrogen generation profile of reaction between $LiBH_4$/MWCNT mixture and water vapor with the continuous increase of temperature from room temperature to 80 °C. The result shows that observable reaction of plain $LiBH_4$ with water

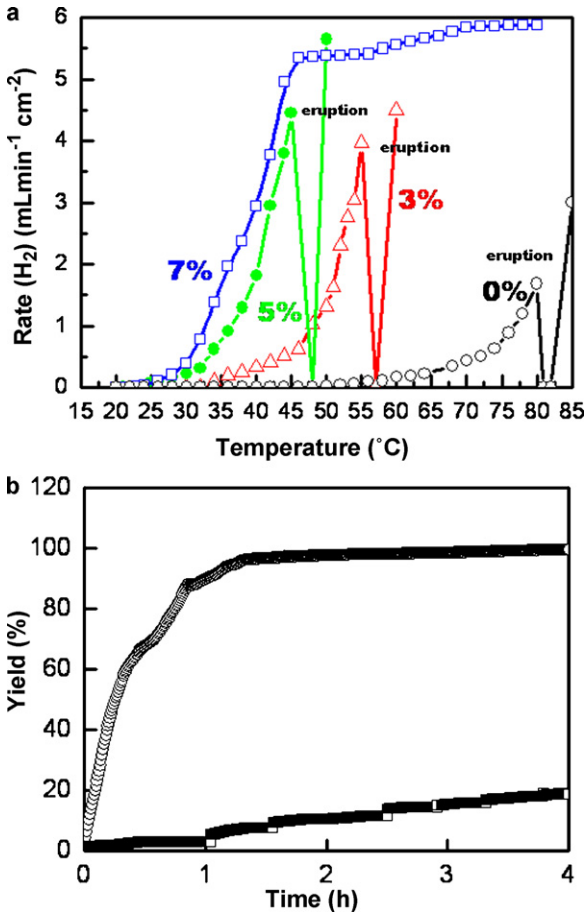

Fig. 7. Hydrogen generation rates of $LiBH_4$ doped with different amounts of MWCNTs (-◯- for 0 wt.%, -△- for 3 wt.%, -●- for 5 wt.% and -□- for 7 wt.% MWCNT addition) with temperature increasing from room temperature to 80 °C at a heating rate of 0.5 °C min^{-1} (a) and hydrogen yield curves of neat $LiBH_4$ (-□-) and $LiBH_4$ doped with 7 wt.% MWCNTs (-◯-) (b).

vapor only takes place at 50 °C, then the hydrogen generation rate rises with temperature increase. When the temperature increases to 80 °C, the hydrogen flow suddenly decreases to zero, and after a few seconds rises suddenly. This phenomenon suggests that the clogging mass of $LiBH_4$ and its solid hydrolysis product prevents the remaining $LiBH_4$ on the top from hydrolysis, which results in a pressure below the product which builds up to a threshold and then breaks the impermeable mass, therefore, a sudden gas eruption is detected.

As for $LiBH_4$ doped with MWCNTs, the initial hydrolysis temperature decreases remarkably and hydrogen evolution rate rises remarkably. When the amount of MWCNTs is smaller than 7 wt.%, the hydrogen evolution rate rises with the increase of MWCNT amount, however, the gas eruption caused by clogging effect of $LiBH_4$ hydrolysis was still observed. When the amount of MWCNTs is 7 wt.%, the hydrolysis of $LiBH_4$ starts from 25 °C, and the hydrogen evolution rate firstly rises rapidly with temperature increasing, then maintains steady when the temperature is higher than 45 °C and finally reaches a steady rate of about 5.9 mL min^{-1} cm^{-2} at 80 °C. Fig. 7b compares the hydrogen yield profiles of neat $LiBH_4$ and $LiBH_4$ doped with 7 wt.% MWCNTs at 60 °C. The reaction of 2.5 g neat $LiBH_4$ with water vapor shows a stepwise curve, which results from the destabilizing hydrogen evolution under the effect of agglomeration, and the total hydrogen yield is only 20% within 4 h. In contrast, $LiBH_4$ doped with 7 wt.% MWCNTs shows a smooth curve, 100% stoichiometric amount of H_2 can be released with in 2 h. The results clearly demonstrate the enhanced effect of MWCNTs

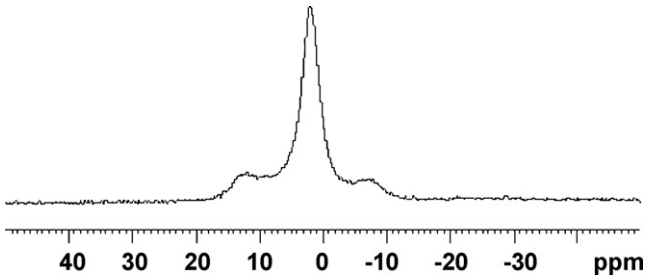

Fig. 8. ^{11}B NMR pattern of condensed hydrolysis product of $LiBH_4$ doped with 7 wt.% MWCNTs.

on the hydrogen generation performance of $LiBH_4$. There is no gas eruption during hydrolysis of $LiBH_4$ doped with 7 wt.% MWCNTs, which indicates that the agglomeration effect of $LiBH_4$ hydrolysis can be avoided by the addition of MWCNTs. Fig. 8 shows the ^{11}B NMR results of condensed hydrolysis product of $LiBH_4$ doped with 7 wt.% MWCNTs. There is no peak at −42 ppm corresponding to $LiBH_4$ [23], which indicates that the hydrolysis reaction of $LiBH_4$ is complete. The peak at 1.8 ppm shows the formation of boric acid, $B(OH)_3$, in good agreement with the NMR results for and BH_4^- hydrolysis [24].

Kong et al. [16] have demonstrated that there was no reaction between water vapor and plain $LiBH_4$ until the hygroscopic borohydride powders effectively "dissolved" and drained into the liquid water at the bottom of the reactor. In our experiments, the opening diameter of stainless steel sieve is much smaller than the milled mixture, and the volume of $LiBH_4$ expands after hydrolysis. In addition, after experiment, no solid product is found in the liquid water below the sieve. Therefore, it is impossible for $LiBH_4$ powder to "drain" into liquid water to yield hydrogen in our case. Because MWCNTs are hollow tubular porous materials, according to the fact of gas adsorption on microporous materials, water vapor accumulates easily on the surface of MWCNTs. At room temperature, MWCNT-doped $LiBH_4$ reacts with the accumulated water vapor resulting in hydrogen yield which can only occur for plain $LiBH_4$ at 50 °C or higher. Furthermore, the experimental results indicate that hydrogen diffuses out from MWCNT-doped $LiBH_4$ more easily than from plain $LiBH_4$. In other words, MWCNTs created gas channels between the mixtures, avoiding gas eruption caused by agglomeration.

The SEM images of the products of plain $LiBH_4$ and 7 wt.% MWCNT-doped $LiBH_4$ are shown in Fig. 9. No pores can be found on the surface of the hydrolysis product of plain $LiBH_4$. The product is a single piece of solid and impermeable mass that can clog the reaction vessel as reported by Zhu et al. [17]. However, the hydrolysis product of MWCNT-doped $LiBH_4$ shows a porous morphology with the diameter of the solid less than 8 μm, which indicates that the product does not form an impermeable mass and that gas can diffuse through the porous structure.

Our results present a novel strategy for fully hydrolyzing $LiBH_4$ by doping with MWCNTs. The hydrolysis of $LiBH_4$ doped with 7 wt.% MWCNTs can quickly release 4 equiv. H_2 and the hydrogen capacity is 7.5 wt.%, suggesting that $LiBH_4$–MWCNT is a promising material for hydrogen source of PEMFCs.

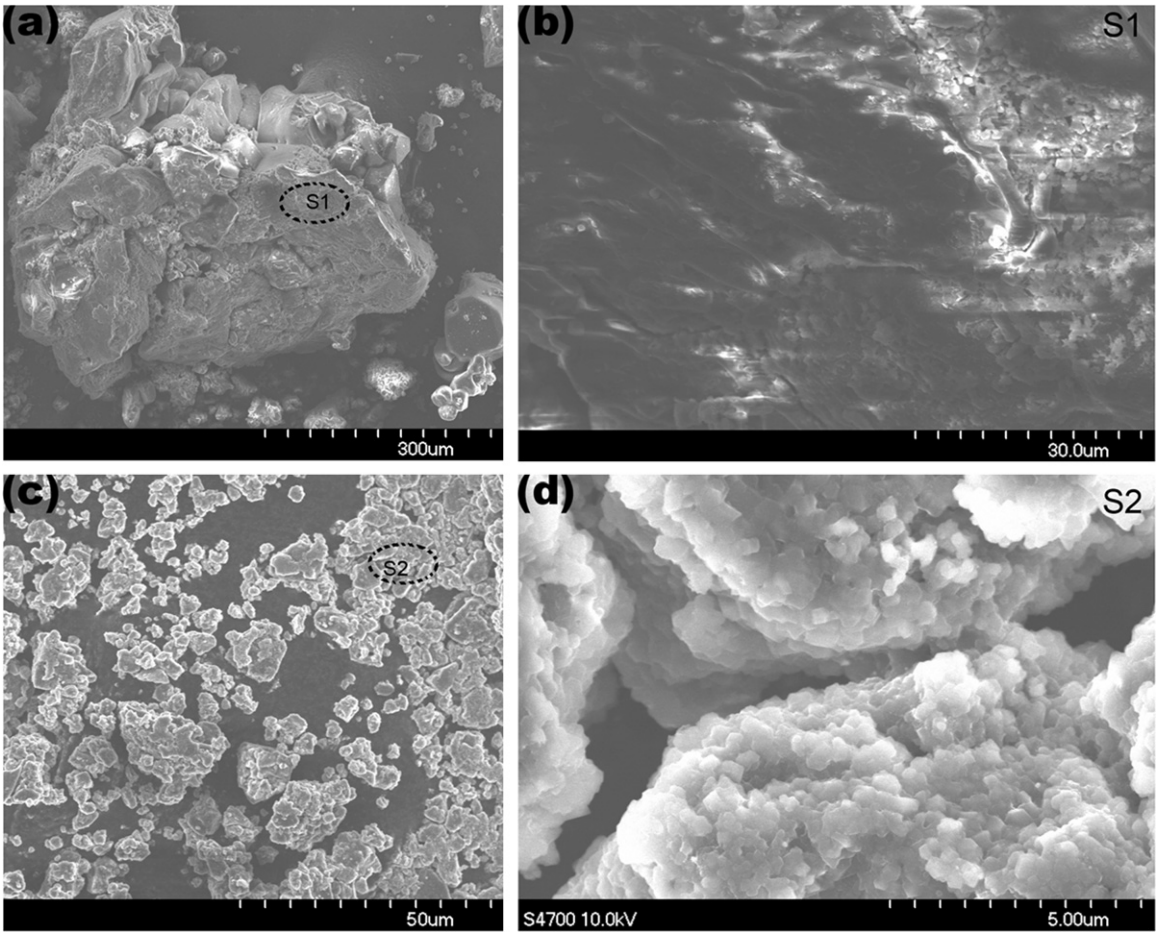

Fig. 9. SEM images of reaction products from hydrolysis reaction of (a) neat $LiBH_4$, (b) amplified images of area S1 in image (a), (c) MWCNT-doped $LiBH_4$, and (d) amplified images of area S2 in image (c).

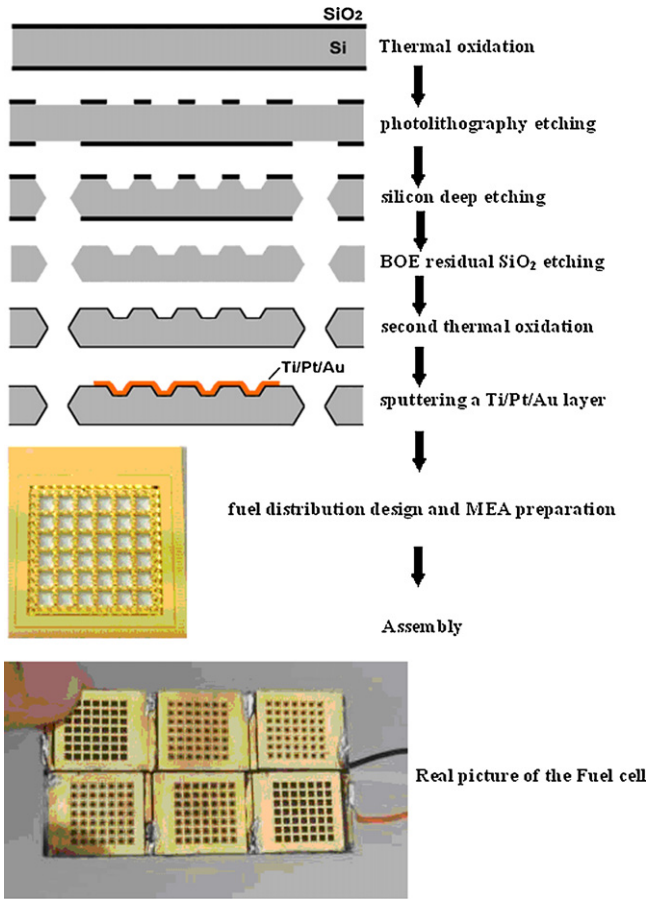

Fig. 10. Schematic of a MEMS micro silicon fuel cell.

Reaction vessel 2 loaded with MWCNT-doped $LiBH_4$ powder was connected to a home-made air-breathing micro PEMFC to test the fuel cell performance with the hydrogen generated from the hydrolysis of MWCNT-doped $LiBH_4$. Details of air-breathing micro-PEMFC fabrication methods have been reported in previous paper [25]. The structure of the hybrid silicon fuel cell is depicted in Fig. 10. Briefly, the fuel cell was manufactured using MEMS fabrication processes. Beginning with a P-type silicon wafer polished on both sides, a 2 μm silicon dioxide layer was grown by wet thermal oxidation. Then photolithography was applied to define the flow channel geometry on the front side and the feed hole geometry on the rear side. The exposed oxide was removed by a buffered oxide etchant (BOE), followed by anisotropic KOH etching down to a channel with depth of approximately 270 μm. After the removal of residue SiO_2 from previous coating by BOE, a new 2 μm silicon dioxide was grown as an insulator layer on the surface by wet thermal oxidation. Metal contact is made by sputtering gold. Nafion solution was painted to fill the channels with a paintbrush. A Pt-based catalyst ink was directly painted on the top of Nafion, and the resulting catalyst loading is approximately 20 mg cm^{-2}. The polarization curve of the fuel cell supplied with hydrogen generated from reacting $LiBH_4$ with water vapor is shown in Fig. 11, with open cell potential about 1 V and maximum power density of 0.15 W cm^{-2}. As shown in Fig. 12, the fuel cell can stably run at 150 mA cm^{-2} for more than 20 h with continuous delivery of hydrogen.

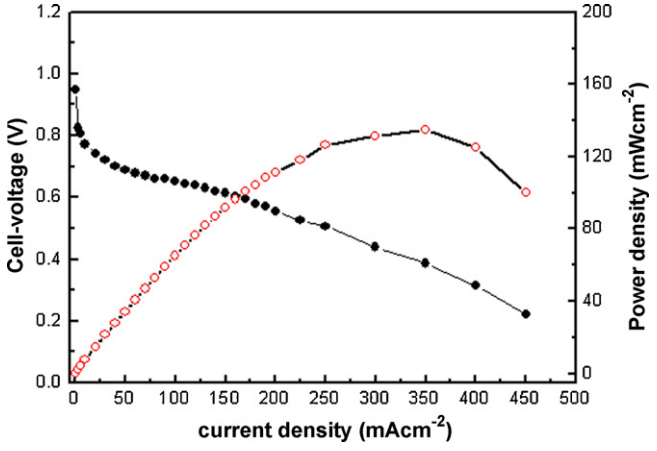

Fig. 11. The polarization curve of a micro PEMFC with hydrogen generated from hydrolysis of $LiBH_4$/MWCNTs.

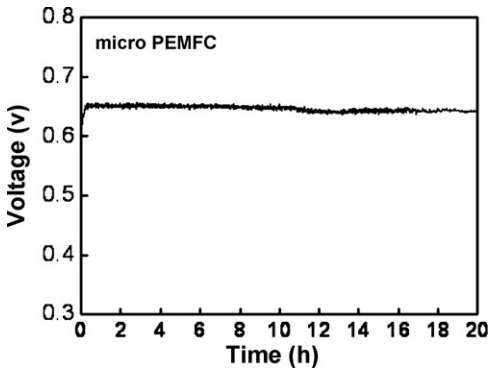

Fig. 12. The fuel cell long-life test curve at 150 mA cm^{-2} with hydrogen generated from $LiBH_4$/MWCNT hydrolysis.

4. Conclusion

In summary, we first investigate the hydrolysis of plain $LiBH_4$ and find the maximum temperature during the hydrolysis process is higher than 80 °C and increases with increasing bulk density of $LiBH_4$ which affects the water consumption and hydrolysis product. Then we demonstrate that full hydrolysis of $LiBH_4$ can be achieved by the addition of MWCNTs. Our result clearly shows that with the addition of MWCNTs, the onset temperature is lowered from 50 °C to room temperature, and hydrogen yield of $LiBH_4$ hydrolysis is stabilized. H_2 diffuses out more easily than plain $LiBH_4$. The addition of MWCNTs created gas channels between the mixtures, avoiding gas eruption caused by agglomeration. The hydrogen capacity is 7.5 wt.% in total. A fuel cell driven by hydrolyzing $LiBH_4$/MWCNT mixture can stably run for more than 20 h, suggesting that $LiBH_4$/MWCNT is a suitable material for the application of hydrogen generation system on PEMFCs.

Acknowledgments

The authors would like to acknowledge the help of Professor Yongting Wang from Shanghai Jiaotong University for revising our manuscript. This work was financially supported by National "863" High-Tech. Research Programs of China (2008AA05Z102) and the SIMIT-QN Innovation Foundation (No. 119900QN04).

References

[1] S.F.J. Flipsen, J. Power Sources 162 (2006) 927–934.
[2] Z.T. Xia, S.H. Chan, J. Power Sources 152 (2005) 46–49.
[3] J. Yeom, R.S. Jayashree, C. Rastogi, M.A. Shannon, P.J.A. Kenis, J. Power Sources 160 (2006) 1058–1064.
[4] W.M. Yang, S.K. Chou, C. Shu, J. Power Sources 164 (2007) 549–554.
[5] J. Yang, A. Sudik, D.J. Siegel, Angew. Chem. Int. Ed. 47 (2008) 882–887.
[6] L. Schlapbach, A. Züttel, Nature 414 (2001) 353–355.

[7] A. Züttel, P. Wenger, S. Rentsch, P. Sudan, Ph. Mauron, Ch. Emmenegger, J. Power Sources 118 (2003) 1–7.
[8] R.L. Cohen, J.H. Wernick, Science 214 (1981) 1081–1087.
[9] G.S. Walker, D.M. Grant, T.C. Price, X.B. Yu, V. Legrand, J. Power Sources 194 (2009) 1128–1134.
[10] P. Chen, Z.T. Xiong, J. Luo, J.Y. Lin, K.L. Tan, Nature 420 (2002) 302–304.
[11] H. Senoh, Z. Siroma, N. Fujiwara, K. Yasuda, J. Power Sources 185 (2008) 1–5.
[12] B.H. Liu, Z.P. Li, J. Power Sources 187 (2009) 527–534.
[13] Y. Kojima, K. Suzuki, Y. Kawai, J. Power Sources 155 (2006) 325–328.
[14] Y. Kojima, Y. Kawai, M. Kimbara, H. Nakanishi, S. Matsumoto, Int. J. Hydrogen Energy 29 (2004) 1213–1217.
[15] L. Laversenne, C. Goutaudier, R. Chiriac, C. Sigala, B. Bonnetot, J. Therm. Anal. Calorim. 94 (2008) 785–790.
[16] V.C.Y. Kong, F.R. Foulkes, D.W. Kirk, J.T. Hinatsu, Int. J. Hydrogen Energy 24 (1999) 665–675.
[17] L. Zhu, D. Kim, H. Kim, R.I. Masel, M.A. Shannon, J. Power Sources 185 (2008) 1334–1339.
[18] K. Deshmukh, K.S.V. Santhanam, J. Power Sources 159 (2006) 1084–1088.
[19] S. Cahen, J.B. Eymery, R. Janot, J.M. Tarascon, J. Power Sources 189 (2009) 902–908.
[20] H.I. Schlesinger, H.C. Brown, A.E. Finholt, J.R. Gilbreath, H.R. Hoekstra, E.K. Hyde, J. Am. Chem. Soc. 75 (1953) 215–219.
[21] M. Diwan, H.T. Hwang, A. Al-Kukhun, A. Varma, AIChE J. 57 (2011) 259–264.
[22] C.H. Liu, B.H. Chen, C.L. Hsueh, J.R. Ku, F. Tsau, J. Power Sources 195 (2010) 3887–3892.
[23] B.C. Weng, X.B. Yu, Z. Wu, Z.L. Li, T.S. Huang, N.X. Xu, J. Ni, J. Alloy Compd. 503 (2010) 345–349.
[24] M. Chandra, Q. Xu, J. Power Sources 156 (2006) 190–194.
[25] J.Y. Cao, Q.H. Huang, Z.Q. Zou, T. Yuan, Z.L. Li, B.X. Xia, H. Yang, J. Power Sources 185 (2008) 433–438.